Applied Catalysis A: General 341 (2008) 26–34

Contents lists available at ScienceDirect

Applied Catalysis A: General

journal homepage: www.elsevier.com/locate/apcata

Deactivation studies of the SCR of NO_x with hydrocarbons on Co-mordenite monolithic catalysts

Alicia V. Boix *, Soledad G. Aspromonte, Eduardo E. Miró

Instituto de Investigaciones en Catálisis y Petroquímica, INCAPE (FIQ, UNL-CONICET), Santiago del Estero 2829, 3000 Santa Fe, Argentina

ARTICLE INFO

Article history:
Received 18 July 2007
Received in revised form 30 November 2007
Accepted 10 December 2007
Available online 7 March 2008

Keywords:
Hydrocarbon-SCR
Monolithic catalysts
CoMOR
Deactivation
Cobalt characterization
UV–vis
Raman

ABSTRACT

The catalytic reduction of NO_x with hydrocarbons (butane or methane) on CoMOR washcoated monolithic catalysts was studied in the presence of steam and excess oxygen. The significant changes observed in the catalytic behavior of CoMOR powder and monoliths depended essentially on the hydrocarbon nature (carbon number) and the concentration of water in the feed. When the reducing agent was methane, a low concentration of water (2%) decreased the NO to N_2 conversion. However, when butane was used instead of methane, the maximum NO_x conversions increased from 50 to 58% and from 52 to 64% for the CoMOR powder and monolith, respectively. The presence of water inhibited the NO adsorption when the reducing agent was methane but when butane was used, water helped to remove the surface-carbon deposits as indicated by TPO and XPS results. This fact explains the increase observed in the NO_x conversion. The characterization with TPR and UV–vis spectroscopy showed that the main Co species present in the selective catalysts were the Co(II) ions exchanged at different sites of the mordenite and highly dispersed Co_xO_y moieties. More rigorous reaction conditions, i.e. 10% of water, led to the irreversible deactivation with both reductants. The Co_3O_4 phase was detected in all the deactivated powder and monolithic catalysts. The Co_3O_4 spinel was formed from the cobalt ion migration, which was promoted in wet atmosphere. In addition, for monolithic catalysts washcoated with CoMOR, the silica binder inhibited the water deactivation effect probably due to the silica–cobalt interaction, as a Co_xO_ySi silicate.

1. Introduction

The catalytic reduction of NO_x using hydrocarbons and in the presence of oxygen excess has been the object of intense research efforts in the last decades [1]. Several powder catalysts have been developed, most of them using zeolites as supports of cations, e.g. Co, Fe, Cu, In [2–5]. Other oxide supports such as ZrO_2 and Al_2O_3 have also been studied [6,7]. Very active catalysts have been reported in the literature but the problem of deactivation under high temperatures and water still remains unsolved in most cases [8,9].

Applications of the NO_x SCR process can be found in stationary sources in which ammonia is used as reductant. However, it is preferable to use hydrocarbon rather than ammonia as reducing agent in order to avoid ammonia tail emissions and other problems associated with the corrosivity of this gas [10].

Another interesting application of this reaction is in internal combustion engines operating with oxygen excess, i.e. diesel and lean burn gasoline engines [11]. However, the difficulty in achieving hydrothermal stability has seriously limited the implementation of zeolite-based NO_x SCR catalysts.

Among the catalysts studied, Co-exchanged zeolites have received considerable attention. Since the pioneering work of Li and Armor [12,13] reporting the activity of Co-ZSM5 in the NO_x reaction with methane under wet conditions, several articles have been published studying mechanistic aspects [14], catalyst characterization [15] and deactivation processes [16]. In a recent work, Martínez-Hernández and Fuentes [17] proposed an irreversible deactivation mechanism during long-time operation periods under wet conditions in the reduction of NO_x by propane on Co-ZSM5. At time-on-stream of the order of 10 h, CoO_x moieties nucleated and then grew to form small crystallites of Co_3O_4 inside the zeolite channels, resulting in the irreversible deactivation of the catalysts. Structural characterizations showed that dealumination was not significant under the conditions employed.

For practical purposes, catalytic powders should be supported on structured substrates such as monoliths. Cordierite is the most widely used material for honeycomb manufacturing given its superior hydrothermal stability, mechanical features and low

* Corresponding author. Tel.: +54 342 4536861; fax: +54 342 4536861.
E-mail address: aboix@fiqus.unl.edu.ar (A.V. Boix).

0926-860X/$ – see front matter © 2008 Elsevier B.V. All rights reserved.
doi:10.1016/j.apcata.2007.12.032

thermal expansion coefficients [18]. However, only a handful of papers concerning the activity and stability of monolithic catalysts for the NO_x SCR with hydrocarbons have been published so far [19,20]. Nonetheless, it is important to study monolithic catalysts since the powder–support interaction can give rise to different behaviors if compared to the unsupported catalysts. This fact has already been demonstrated in the literature; Boix et al. [21–23] reported that the binders commonly used to firmly attach the catalyst washcoat to the cordierite honeycomb strongly affect the catalytic behavior. When silica is used as a binder for a PtCo Ferrierite washcoat, the NO_x conversion rate improves as well as the resistance to deactivation under wet atmosphere. This behavior is attributed to the interactions between hydrophobic silica particles and zeolite crystals [21]. However, when $Al(NO_3)_3$ is used as binder, the formation of a non-stoichiometric spinel $Co_xAl_yO_4$ provokes a strong deactivation of the catalyst [22]. Li et al. [23] studied metal-MFI/cordierite for the SCR of NO_x by propane. They found that when the in situ synthesis method is used, a strong interaction develops between the zeolite and the substrate, leading to an improved hydrothermal stability of the zeolite.

In a recent study, Zamaro et al. [24], using Fe–Cr alloy monoliths as substrate, have shown that oriented films of In-mordenite result in catalysts with higher activity than the powder.

Thus, it has been demonstrated that the catalytic behavior cannot be extrapolated from powder catalysts results to those of monolithic catalysts because the interactions with the substrate and/or with binders can strongly affect both the catalytic activity and the hydrothermal stability. Accordingly, the aim of this work is to study the behavior of a Co-mordenite/cordierite catalyst for the catalytic reduction of NO_x with methane and butane in oxygen excess. To this end, catalytic tests and deactivation studies have been performed together with a thorough characterization of fresh and used catalysts by means of temperature-programmed reduction experiments (TPR), laser Raman spectroscopy (LRS), UV–vis diffuse reflectance spectroscopy (DRS), and X-ray photoelectron spectroscopy (XPS).

2. Experimental

2.1. Preparation of Co-mordenite powder catalysts

Catalysts were prepared by ion exchange starting from commercial Na-mordenite (Zeolyst CV10A, $SiO_2/Al_2O_3 = 13$). The cobalt-exchanged Na-mordenite (CoMOR) solids were prepared using a cobalt acetate solution (0.025 M), with a ratio of 10 g zeolite in a 1.5 l solution. The exchange time was 24 h at 50 °C, (pH 5–6) and then the solids were filtered, washed, and dried at 120 °C for 8 h. The sample was calcined at 400 °C for 2 h, in O_2 flow at a slow heating rate (2 °C min^{-1}). The CoMOR catalyst contained 3 wt.% of cobalt.

2.2. Preparation of washcoated monolithic catalysts

A suspension with ca. 25 wt.% of CoMOR (in deionized water) was used to impregnate a cordierite support (Corning) having square-section cells with a density of 400 cells/in^2. Three successive immersions of the monolith in the suspension (pH 6) were performed to achieve the expected zeolite load (approximately 20 wt.% on a dry basis). It was performed with or without the addition of a binder (cab-o-sil, surface area = 200 m^2 g^{-1}; particle diameter = 5–30 nm). After each immersion (ca. 10 s), air was softly blown to eliminate the excess suspension to achieve a homogeneous film on the ceramic surface. It was dried at 120 °C overnight, and then calcined in oxygen flow at 400 °C for 2 h.

2.3. Catalytic measurements

The catalysts were evaluated in a continuous flow system. The typical composition of the reacting stream was the following: 1000 ppm NO, 500 ppm C_4H_{10} or 1000 ppm CH_4, 2% O_2, balanced at 1 atm in helium (Gas-hourly space velocity, GHSV = 20,000 h^{-1}). The washcoated monoliths, (1 cm × 1 cm × 2 cm) were placed in the same reactor between two quartz wool plugs, and the quartz tube was filled with CSi particles to avoid bypass flow. The GHSV is defined as flow rate × zeolite apparent density/zeolite weight. In this way, the catalytic results obtained with washcoated monoliths can be compared to those of powder zeolites. In some runs, water was also introduced in the feed in order to test the deactivation behavior of the best formulations.

The gases were analyzed with an SRI 9300B chromatograph equipped with a 5A molecular sieve column at room temperature and the carrier gas was He. The NO_x conversion (C_{NO}) was calculated as $C_{NO} = 2 \times 100([N_2]/[NO]^\circ)$, where $[NO]^\circ$ is the NO initial concentration. The hydrocarbon (HC) conversion (C_{HC}) was obtained as $C_{HC} = 100([HC]^0 - [HC])/[HC]^0$.

The composition of the reactor effluent was also monitored for CO, NO, NO_2, N_2O, CH_4 or C_4H_{10} using a Fourier transform infrared spectrometer (FTIR), Thermo Matso Genesis II, equipped with a gas IR cell having a 15 cm path length (47 ml volume). A total of 100 scans were collected with a nominal resolution of 1 cm^{-1}.

2.4. Carbon deposits characterization

The amount and characteristics of the carbon deposited during the NO_x SCR reaction with butane were determined by temperature-programmed oxidation (TPO) and X-ray photoelectron spectroscopy (XPS). In this way, two aliquots of calcined CoMOR powder were used for 10 h at 400 °C under reaction conditions with and without 2% H_2O, respectively. The TPO experiments were carried out using 20 mg of catalyst dehydrated in situ at 300 °C in N_2 flow. A gaseous flow with 6% O_2 in N_2 was used and the temperature was increased at a rate of 12 °C/min.

XPS analyses were performed in a multi-technique system (SPECS) equipped with a dual Mg/Al X-ray source and a hemispherical PHOIBOS 150 analyzer operating in the fixed analyzer transmission (FAT) mode. The spectra were obtained with a pass energy of 30 eV; an Al Kα X-ray source was operated at 200 W and 12 kV. The working pressure in the analyzing chamber was less than 5×10^{-9} mbar. The Si 2p peak at 103.0 eV binding energy (BE) was taken as internal reference. All the peaks were fitted by a Gaussian–Lorentzian component wave-form after an inelastic (Shirley-type) background had been subtracted in order to calculate the surface atomic ratio.

2.5. TPR experiments

These experiments were performed using an Okhura TP-2002 S instrument equipped with a TCD detector. The reducing gas was 5% H_2 in Ar, flowing at 30 ml min^{-1} and the heating rate was 10 °C min^{-1} up to 900 °C. Fresh samples were pre-treated in situ in flowing O_2, heating at 2 °C min^{-1} up to 400 °C and kept at that temperature for 2 h. The amount of CoMOR powder used was 0.05 g and 0.2–0.25 g in CoMOR monolith crushed into small pieces. The H_2 consumption is not referred to the cobalt content of the monolith samples (as in the case of powder samples) due to some uncertainty about it.

2.6. Raman spectroscopy

The Raman spectra were recorded with a TRS-600-SZ-P Jasco Laser Raman instrument, equipped with a CCD (change-coupled

device) with the detector cooled to about 153 K using liquid N_2. The excitation source was the 514.5 nm line of a Spectra 9000 Photometrics Ar ion laser. The laser power was set at 30 mW. For Raman spectroscopy the powder sample, calcined and used, was pressed at 4 bar into self-supporting wafers and the monolith samples were used as they had been prepared and after use in the catalytic test.

2.7. UV–vis spectroscopy

Diffuse reflectance spectroscopy (DRS) studies in the ultraviolet–visible (UV–vis) region were made using a Varian Cary 5 E spectrometer, with an optical accessory (Praying Mantis, Harrick) and a high-temperature reaction chamber. The samples were dehydrated in flow of N_2 (30 cm^3 min^{-1}) using a temperature rate of 10 °C min^{-1} up to 450 °C; this temperature was kept constant during 30 min. The spectral data were acquired with a 0.5 nm resolution at room temperature. The spectrum of the dehydrated parent zeolite was subtracted from those of the catalysts in order to observe only the cobalt contributions.

3. Results and discussion

3.1. Catalytic behavior

The CoMOR powder catalyst and supported on cordierite monoliths, calcined in O_2 at 400 °C, was studied in the selective reduction of NO_x with two different hydrocarbons, butane or methane, under dry and wet reaction conditions.

The samples were analyzed between 300 and 500 °C. The maximum NO to N_2 conversions reached with the CoMOR powder catalyst (at 400 °C) using butane were 51% (dry) and 58% when 2% H_2O was added to the feed stream (Fig. 1A). In both cases, the butane conversion was 100% at 400 °C.

Then the catalyst was evaluated during isothermal dry/wet conditions at 400 °C (Fig. 1B). During the first 45 min of isothermal reaction in wet flow, the NO conversion decreased from 58 to 45%. After that, it began to increase, reaching 62% after 2 h on stream (Fig. 1B). The transient behavior observed during the first stage of the experiment could be ascribed to different phenomena taking place in the catalyst, i.e. cobalt ions redistributions inside the zeolite structure [17], carbon formation and carbon removal assisted by water. When the water in the feed was removed, the N_2 conversion decreased to 53% and remained constant. During the following 20 h, the NO average conversion was 60% at 400 °C in wet feed.

After these treatments (24 h), the effluent flow reactor was analyzed by FTIR spectroscopy. Butane and NO conversions and NO_x species concentrations vs. temperature are shown in Fig. 1C and D. Note that the NO_2 concentration was less than 130 ppm under wet conditions and N_2O was not detected. Simultaneously, the N_2 concentration was measured by GC, which completed the nitrogen balance.

Fig. 2 and Table 1 show the catalytic performance of the CoMOR powder and the two monoliths (CoMOR-M) prepared with and without ca. 1 wt.% colloidal silica added in a washcoating slurry during the preparation step. The reducing activity of CoMOR-M was higher than the CoMOR powder and the maximum NO to N_2 conversion was 58% (without SiO_2) and 64.3% (with SiO_2) under wet feed (Fig. 2B) at 400 °C. When the water concentration increased to 10%, the maximum NO to N_2 conversion with CoMOR-M (+SiO_2) dropped to 17–18% (see Table 1).

The hydrothermal stability for both monoliths was studied at constant temperature (400 °C) adding 2% H_2O. The NO to N_2 conversion remained around 55% (without SiO_2) and 63% (with SiO_2) after 10 h of time-on-stream. After that, in the most selective catalyst CoMOR-M(+SiO_2), the water concentration in the feed was increased to 10% and the NO to N_2 conversion was around 15% during the next 10 h. The catalyst deactivation was partially reversible because when water was decreased to 2% H_2O, the conversion hardly reached 30% (400 °C), progressively decreasing to 13%.

In order to compare the reducing activity of CoMOR with methane as reductant, the CoMOR-M monoliths were catalytically evaluated using similar reaction conditions for CH_4-SCR. The maximum NO to N_2 conversion was 33% for CoMOR-M and 20% for CoMOR-M(+SiO_2) at 475 °C and 20,000 h^{-1}, whereas the CH_4 conversion was 80% for both samples. In a previous study made with powder catalysts [25], we found that the maximum NO to N_2 conversion for CoMOR (2.9% Co) was 30% at GHSV = 6500 h^{-1} and 17% at GHSV = 30,000 h^{-1}, respectively, under similar reaction conditions: 450 °C, CH_4/NO = 1 ratio and dry feed stream. Therefore, the samples supported on monolith have a better reducing activity than the powder CoMOR catalyst.

3.2. Characterization of Co species

Figs. 3 and 4 show the temperature-programmed reduction results for CoMOR (powder) and CoMOR-M washcoated monoliths, respectively. The H_2 consumption per mol of Co for CoMOR (powder) and the (peak area/total area) ratio for CoMOR-M are summarized in Table 2.

The TPR profile of the calcined CoMOR (Fig. 3, profile a) presents a broad peak between 200 and 500 °C and another one with a maximum at 687 °C. For temperatures lower than 500 °C, the H_2 consumption per mol of Co indicates that 22% of the total cobalt is reduced in this area, while at higher temperatures, the degree of the reduction reaches 47%. The first peak could be assigned to a fraction of the cobalt supported as oxide species (CoO_x) while the maximum at 687 °C may be due to the Co^{2+} ions reduction at exchange position inside the framework. The used CoMOR profile (Fig. 3, profile b) is compared to the fresh sample, where the first peak is now well defined with a maximum at 227 °C and the percentage of Co^{2+} ions reduction, at 656 °C, increased to 76% (Table 2). This profile corresponds to CoMOR powder after use with 2% H_2O in the feed stream for 30 h, in which the NO to N_2 conversion remained around 60% (see Fig. 1B). The calcined CoMOR powder prepared with added 1% SiO_2 showed a smaller H_2 consumption than without SiO_2 in the full temperature range (see Table 2).

Fig. 4 shows the TPR data obtained for CoMOR-washcoated monoliths, calcined (Fig. 4A) and after use on wet reaction conditions at 400 °C with butane (Fig. 4B). The data presented in Table 2 are in the form of H_2 consumption percent of each peak. They are not referred to the Co content of the sample due to the uncertainly about the Co content of monolithic portion samples. The TPR profiles of calcined CoMOR-M (with and without SiO_2) show two reduction regions similar to those unsupported samples, the only difference being a shift to lower temperatures of the peak corresponding to exchanged Co ions, probably due to their location in more accessible positions. After the catalysts were under wet reaction conditions, the profiles exhibited an increase on the higher temperature area. The CoMOR-M(+SiO_2) catalyst, deactivated on 10% stream for 10 h, shows a markedly different TPR profile (see Fig. 4B profile e) in which the peak of Co ions at exchange sites strongly decreases due to the formation of Co_3O_4. The latter species is responsible for the peak at 391 °C. The formation of Co oxide and the depletion of Co-exchanged active sites originate the deactivation of the catalyst. A sample without SiO_2 deactivated under the same conditions shows a similar TPR profile.

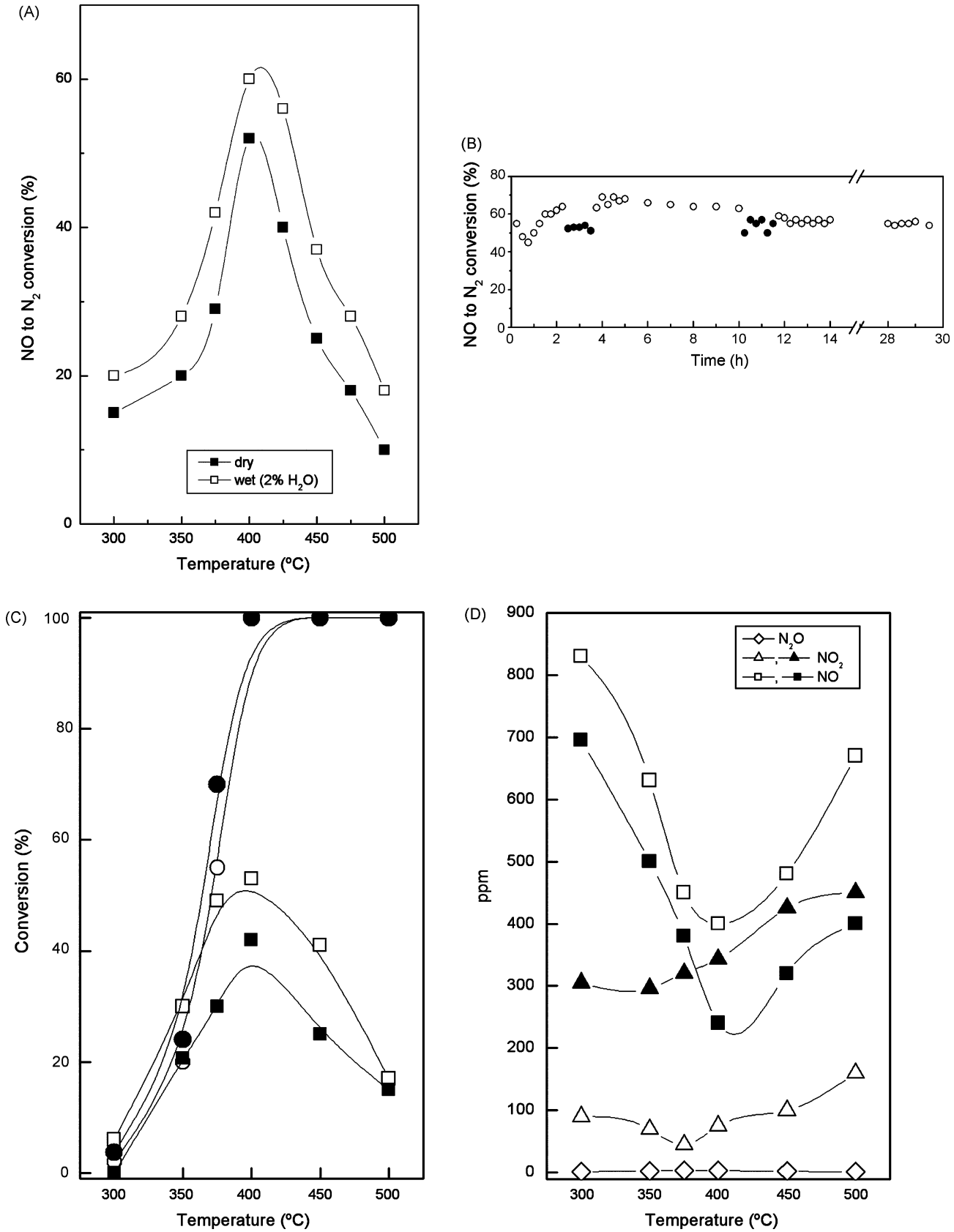

Fig. 1. The SCR of NO_x using CoMOR powder. Reaction conditions: GHSV = 20,000 h^{-1}, 500 ppm C_4H_{10}, 1000 ppm NO, 2% O_2. Filled symbols, dry conditions; empty symbols, wet conditions (2% H_2O). (A) NO_x to N_2 conversion as a function of temperature. (B) Variation of NO_x to N_2 conversion in time-on-stream at 400 °C. (C) NO_x to N2 (■, □) and butane (●, ○) conversions of CoMOR powder, after 24 h of isothermal cycles. (D) NO_x species concentrations as a function of temperature for the SCR of NO_x on the CoMOR powder.

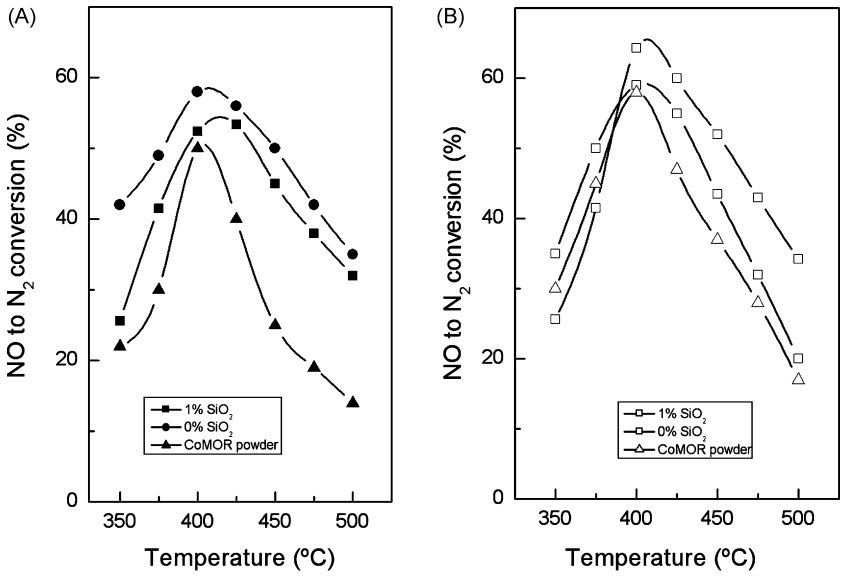

Fig. 2. NO_x to N_2 conversion as a function of temperature for the SCR of NO_x of the CoMOR powder and CoMOR-monoliths. Reaction conditions: GHSV = 20,000 h^{-1}, 500 ppm C_4H_{10}, 1000 ppm NO, 2% O_2. (A) Dry conditions and (B) wet condition, 2% H_2O.

Fig. 5 presents the Raman spectra of calcined CoMOR (powder), NaMOR reference, and used CoMOR-monolith catalysts. NaMOR exhibits several Raman bands at 636, 515, 458 (broad), 400 and 350 cm^{-1} (spectrum a). The spectra of CoMOR (spectrum b) calcined at 400 °C present the bands corresponding to the NaMOR zeolite only. After use in the NO_xSCR with water, all the catalysts (CoMOR powder, CoMOR-M and CoMOR-M + SiO_2) present an additional weak band at 684 cm^{-1}, which corresponds to the main signal of Co_3O_4 (see Fig. 5, spectra c, d, and e). The other bands that are characteristic of Co_3O_4 are not well developed due to the low amount of oxide concentration. However, after using the monolith for 20 h with 2 and 10% of water, spectrum (f) shows the completely developed Co_3O_4 spinel phase with bands at 689, 520 and 480 cm^{-1}. Jongsomjit and Goodwin [26] assigned these bands to the spinel phase and they also reported other bands at 619 and 198 cm^{-1}.

Figs. 6 and 7 show the UV–vis spectra of CoMOR powder and monolith catalysts, calcined and after use under reaction conditions. The absorption spectra in the vis region of Co-exchanged-mordenite are used for description of Co species localized in the cationic sites of the mordenite structure.

Fig. 6 shows UV–vis spectra of CoMOR (powder), calcined at 400 °C, CoMOR plus 1% SiO_2 (washcoating slurry) and CoMOR after use under wet reaction conditions. In all cases, we found a three-band absorption pattern with bands around 500, 580 and 650 nm. The spectra we observe are similar to those reported and deeply discussed by Wichterlova and co-workers [27,28] for Co ions exchanged in different zeolites (mordenite, ferrierite and ZSM-5). This triplet is distinctive of the d–d transitions of Co(II) ions in the tetrahedral coordinations.

Table 1
Effect of water addition upon NO conversion on CoMOR-Monolith(+SiO_2)

T (°C)	NO to N_2 conversion (%)		
	0% H_2O	2% H_2O	10% H_2O
300	15.6	20.0	12.8
350	25.6	26.1	18.3
400	52.4	64.3	17.6
450	45.0	52.0	11.6
500	32.0	35.0	5.4

Dědeček and Wichterlova [28] studied the Co^{2+} ion sitting on a pentasil zeolite and found three different site-coordinations in dehydrated mordenite which can be summarized as follows: different spectral components can be connected to three Co species localized in cationic sites of the mordenite structure. Component α is characterized by the absorption band at 15,000 cm^{-1} (660 nm); a complex asymmetric band with a maximum at 16,500 cm^{-1} (593 nm) represents component β; and two bands at 20,000 (500 nm) and 22,000 (454 nm) are characteristic of component γ. The alpha-type Co ions are coordinated to the walls of the main channel of the mordenite. The beta-type Co ions are suggested to be coordinated to framework oxygens of the twisted eight-member rings of the mordenite cavity. The γ-type Co ions are in the so-called "boat-shaped" site of the mordenite.

Starting from the measured UV–vis spectra (Fig. 6) and the values of the maxima detailed in the Table 3, it is difficult to define a preferential cationic site at which the cobalt ions are located since possibly the three sites (α, β, γ) are partially occupied by the present cations. It would be necessary to use the assignments and adsorption coefficients reported by Wichterlova [27,28] in order to determine the relative population of the Co^{2+} ions through the spectra deconvolution.

Moreover, a weak shoulder at 380 nm is observed on the calcined and used CoMOR samples (Fig. 6). According to the literature, the absorption bands at 380 and 710 nm are assigned to the spinel structure of Co_3O_4, which is composed of Co(II) and Co(III) ions in tetrahedral and octahedral coordinations, respectively [29]. However, the features between 300 and 350 nm can be assigned to Co^{3+} in a distorted tetrahedral environment or to a portion of the Co species outside the framework. Usually, the band around 250 nm (UV region) results from oxygen to metal charge transfer [30].

The CoMOR washcoated monoliths showed similar spectra, since the measured bands on calcined CoMOR-M were the triplets at 500, 570, 635 nm, caused by the absorption transition of tetrahedrally coordinated Co(II) ions and a shoulder at 400 nm. In the catalysts prepared without SiO_2, an additional weak band was observed at 760 nm. Fig. 7 shows the UV–vis spectra of monolithic catalysts, which are used under wet reaction conditions (2–10% water). In the active and selective solids, when they are used with 2% of water, we observed bands corresponding to the triplet (at 500, 570, and 630 nm), and other weak shoulders at 400 and

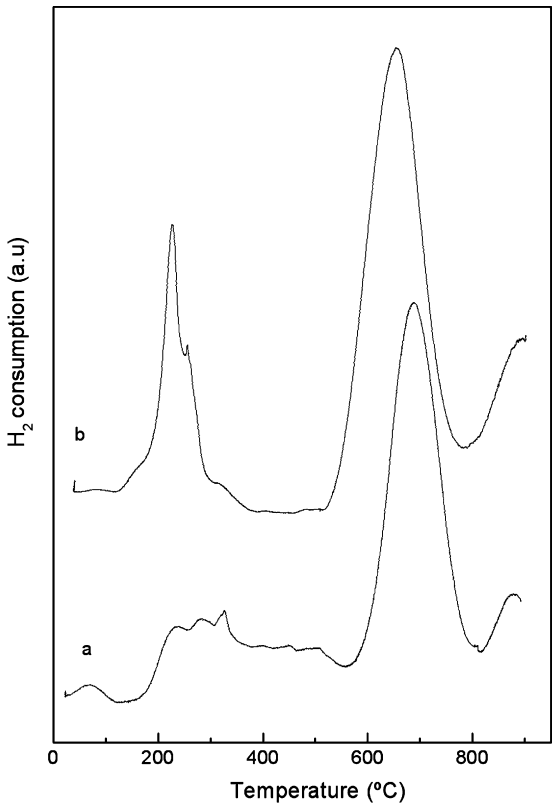

Fig. 3. TPR of CoMOR powder: (a) calcined in O_2 flow at 400 °C and (b) after used for 30 h at 400 °C on C_4H_{10}-SCR with 2% H_2O.

760 nm (Co_3O_4 spinel). The UV–vis spectrum drastically changed after the CoMOR-M + SiO_2 was deactivated under reaction conditions with 10% water, now showing two very broad bands centered at 440 and 720 nm which are characteristic of the Co_3O_4 spinel.

3.3. Effect of water and deactivation

From the catalytic results obtained in this work for Co-mordenite catalysts and other already published ones, it can be inferred that the presence of water in the feed has different consequences depending upon the reaction conditions and the reducing agent being used: (i) water has beneficial effects: it helps maintain the surface clean from carbon deposits and/or it can cause a favorable redistribution of cobalt-exchanged species, (ii) water reversibly inhibits catalytic reaction: it adsorbs at the Co^{2+} active sites preventing the NO_x adsorption, and (iii) it contributes to deteriorate the zeolite microstructure. Consequently, Co ions are released from exchange sites forming both CoO_x moieties and Co_3O_4 crystals. The last effect irreversibly depletes the catalytic activity for NO_x reduction. The listed phenomena have been previously reported in the literature [31].

Schichi et al. [32] studied the effect of carbon number in hydrocarbon reductant on the SCR of NO_x. They found that the effect of carbon number in the region of lower hydrocarbons is the increase in activity when the carbon number increases, such effect being explained by the reactivity of hydrocarbons. In the region of higher hydrocarbons, on the other hand, the SCR activity decreased with an increasing carbon number due to the formation of carbon deposits. Thus, a volcano shaped curve is obtained when NO conversion into N_2 is plotted against Carbon number in *n*-alkane. Under dry conditions the maximum conversion corresponds to butane, and in wet conditions *n*-hexane is the better hydrocarbon.

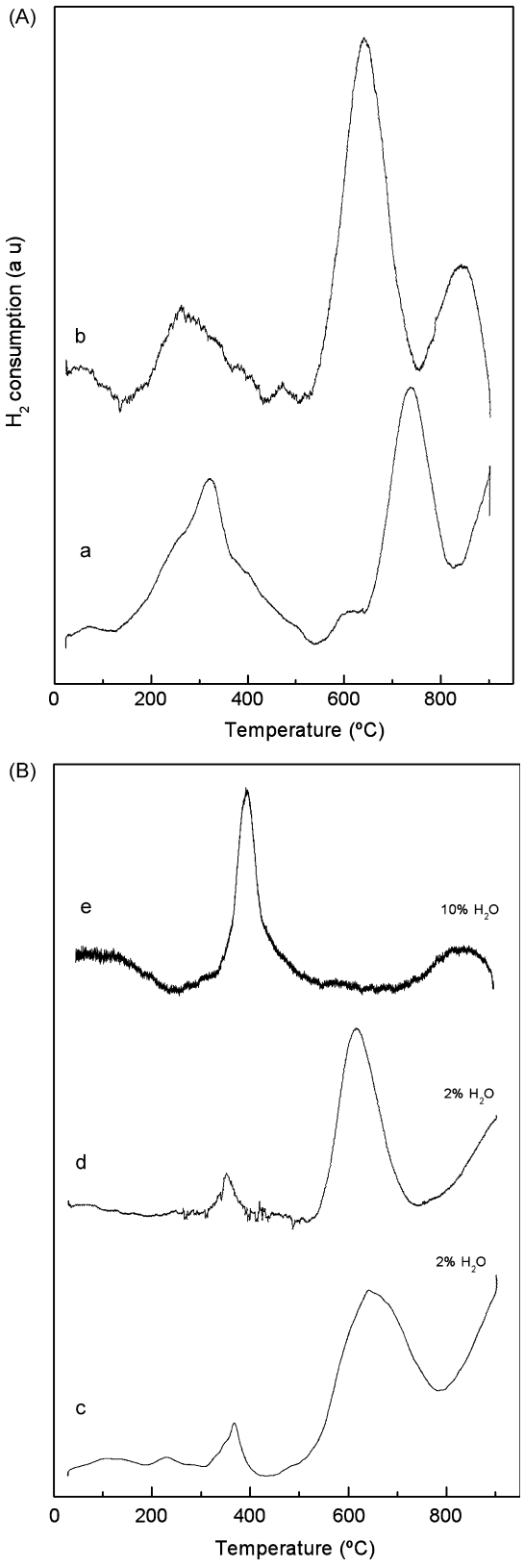

Fig. 4. TPR of CoMOR-M monoliths: (A) calcined at 400 °C; (B) after use at 400 °C for 10 h on C_4H_{10}-SCR with H_2O (2 or 10%). Profiles (a) and (c) monolith washcoated without SiO_2; profiles (b), (d) and (e) monolith washcoated with 1% SiO_2.

Table 2
Reducibility of CoMOR powder and monolithic catalysts

CoMOR powder pretreatment	T_{max} (°C) H_2 consumption/Co (molar ratio)		
O_2, 400 °C	311 (broad) 0.22	687 0.47	–
With 1% SiO_2 O_2, 400 °C	280 0.13	657 0.34	844 0.11
Used C_4H_{10}-SCR 2% H_2O, 400 °C, 30 h	227 0.20	656 0.76	–
CoMOR-M pretreatment	T_{max} (°C) Peak area/total area		
O_2, 400 °C	321 0.48	–	736 0.52
With SiO_2 O_2, 400 °C	308 0.27	658 0.73	
Without SiO_2 Used C_4H_{10}-SCR 2% H_2O, 400 °C, 10 h	368 0.25	643 0.75	
+SiO_2 Used C_4H_{10}-SCR at 400 °C 2% H_2O (10 h)	354 0.13	616 0.87	
+SiO_2 Used C_4H_{10}-SCR at 400 °C 2% H_2O (10 h) + 10% (10 h)	391 0.90		847 0.10

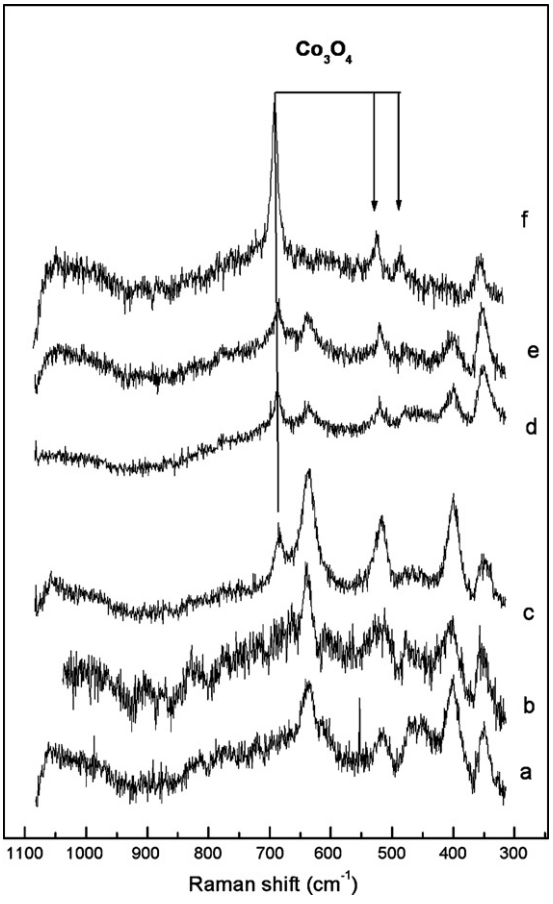

Fig. 5. Raman spectra of NaMOR (a), calcined CoMOR powder (b), CoMOR powder used with 2% H_2O (c), selective CoMOR-M monoliths (without (d) and with SiO_2 (e)) used with 2% H_2O, non-selective CoMOR-M used with 10% H_2O.

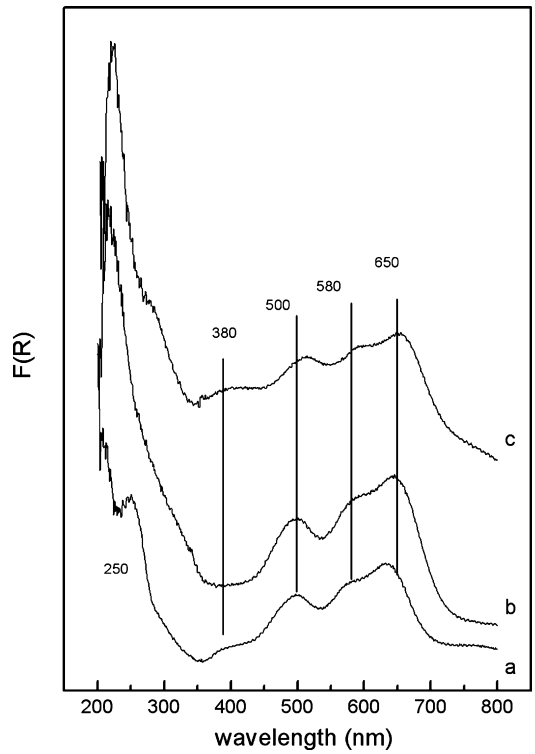

Fig. 6. UV–vis DRS spectra of CoMOR powder: calcined (a), with 1% SiO_2 calcined (b) used under reaction conditions with 2% H_2O (c).

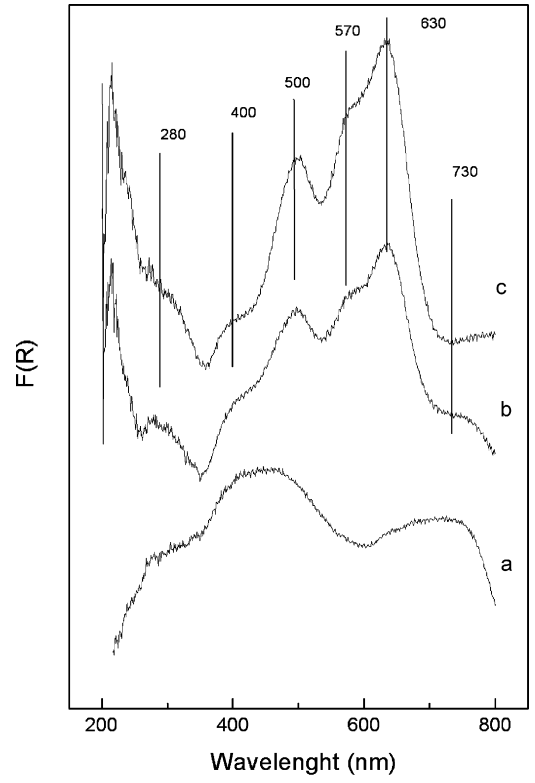

Fig. 7. UV–vis DRS spectra of CoMOR-M monoliths used under wet reaction conditions: CoMOR-M + SiO_2 used with 10% H_2O, unselective catalysts (a); CoMOR-M (b) and CoMOR-M + SiO_2 (c) used with 2% H_2O selective catalysts.

Table 3
Wavelengths of UV–vis spectra of cobalt species on the CoMOR powder and monolithic catalysts

Catalysts	Transition wavelength (nm)				
CoMOR calcined	640	574	500	380	
CoMOR + SiO_2 calcined	645	580	500	–	
CoMOR used	655	580	513	380	
CoMOR-M calcined	635	570	500	400	760[a]
CoMOR-M used active-selective	630	570	500	400	760[a]
CoMOR-M deactivated	–	–	–	440	720

[a] The band at 760 nm was detected on CoMOR-M catalysts washcoated without SiO_2.

Under the conditions used in the cited work [32] NO_x conversion in the absence of water is ca. 20% for ethane, 55% for propane and 65% for butane, indicating that the deposition of carbon starts to be somewhat important for butane. Under wet conditions conversions are ca. 3% for ethane, 20% for propane, 42% for butane and 70% for hexane, suggesting that carbon deposition effect is not important for *n*-alkanes with carbon number below 6.

The above results and those obtained in this work indicate that, when butane is used as hydrocarbon, the carbon cleaning effect of water prevails over the adsorption inhibition one. As a matter of fact, maximum NO_x conversion increases from 50 to 58% and from 52 to 64% when 2% water is added in the feed, for powder and monolithic catalysts, respectively. After several dry/wet cycles at 400 °C, the irreversible deactivation starts and the NO_x conversion slightly decreases. When the water concentration is increased up to 10%, the irreversible deactivation dominates and NO_x conversion is strongly diminished, reaching 4 and 13% for powder and monolith, respectively. It should be noted that the above results for monolithic catalysts correspond to those in which 1 wt.% SiO_2 was added as binder of the CoMOR washcoat.

In order to further study the cleaning effect of water, the carbon deposits were analyzed using TPO and XPS techniques. Both techniques clearly indicate that the amount of carbon is smaller after reaction under wet conditions, thus confirming that the beneficial effect of water in catalytic activity is originated in the cleaning effect.

The TPO measurements in Table 4 corresponding to the CoMOR catalysts after being used for 10 h under dry conditions show a carbon deposition almost twofold that of the catalyst used with 2% H_2O.

Fig. 8 displays C 1s spectra for CoMOR calcined and used under SCR conditions. A main contribution is located at BE of about 285.0 eV; this peak can be assigned to adventitious carbon [33]. The adventitious carbon on the sample surface may originate from atmosphere, sample handling or contamination in the XPS chamber. The distinct peak at 281.2 eV corresponds to deposited carbon species of the graphite type which appear after the catalysts were used. The C/Si surface ratio calculated from XPS data indicate that more carbon is deposited under dry conditions than under wet conditions.

Another effect of water could be the modification of acid properties of the solids. However, our catalysts were prepared from Na-mordenite, thus the presence of Brönsted acid sites are negligible. On the other hand, if some acid sites are formed under reaction conditions with water, the effect of those in reaction rate should be negligible.

Table 4
Carbon characterization deposited on CoMOR powder used in C_4H_{10}-SCR

Reaction conditions[a]	wt.% carbon from TPO (T_{max})	C 1s graphite/Si 2p surface ratio from XPS data
Dry	0.11 (420 °C)	0.70
2% H_2O	0.06 (395 °C)	0.19

[a] Reaction conditions: 400 °C for 10 h, GHSV = 20,000 h^{-1}, 500 ppm C_4H_{10}, 1000 ppm NO, 2% O_2.

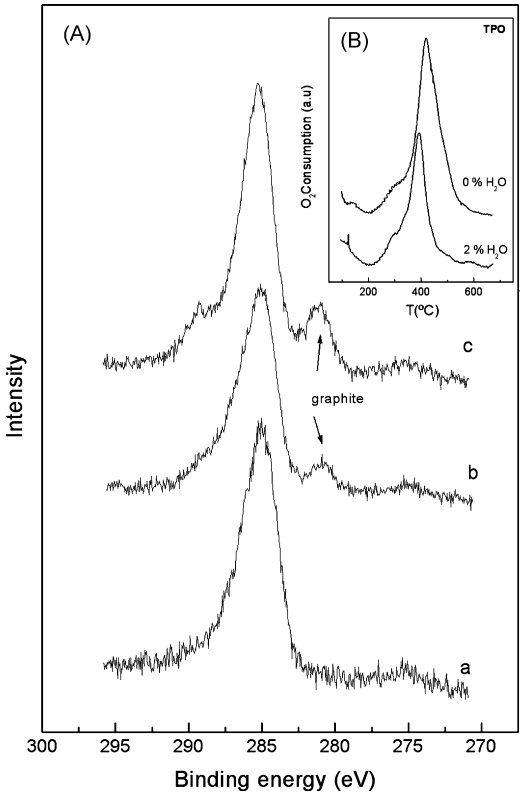

Fig. 8. Carbon deposits on CoMOR powder used 10 h at 400 °C; reaction conditions, see Fig. 2. (A) C1s XPS spectra: (a) calcined at 400 °C, (b) used with 2% H_2O, (c) used without H_2O. (B) TPO results.

3.4. Effect of the silica binder

It is worth noticing that under all conditions, the monolithic catalyst behaves better than the powder one if the comparisons are made loading the same zeolite weights in the reaction experiments. And, on the other hand, the silica binder has a beneficial effect on the activity under wet conditions, but the opposite occurs in the absence of water in the feed (see Fig. 2). When methane is the reductant and under dry conditions, a similar behavior is observed. Thus, we will discuss both the effect of supporting the powder in a monolith and the effects of the silica binder.

The better catalytic performance under dry conditions (see Fig. 2) of our monolithic catalyst, would be attributed to the zeolite–cordierite interactions. In this vein, Li et al. [23] have found that zeolites with MFI structure grown on the surface of honeycomb cordierite substrates have better hydrothermal stability than the powder samples.

However, the zeolite loading in the present work is relatively high so that the portion of the zeolite that closely contacts the cordierite should be rather small. Thus, in our monolithic catalyst, the good flow distribution improved by the monolithic structure could be the origin of the better performance, rather than zeolite cordierite interactions.

As said before, the incorporation of SiO_2 is a positive effect activity under wet reaction conditions. We found a similar result with the PtCo Ferrierite catalyst deposited onto a cordierite monolith [21], the mechanical stability also being improved. In

that work we suggested that an intimate contact between silica and zeolite crystals could occur by which the formation of non-selective species Co_3O_4 is inhibited. We proposed that the surface chemistry of CAB-O-SIL fumed silica is important and may be responsible for the phenomenon observed. Due to hydroxyl groups attached to silicon atoms on the surface of the particles, the fumed silica is capable of hydrogen bonding with zeolite crystals during the slurry process. The small particle size of this material (5–30 nm) makes that phenomenon feasible thus impairing Co coalescence on the zeolite outer surface.

Another effect produced by silica may be the reaction with the deleterious cobalt oxide species to give either crystal cobalt silicate (Co_2SiO_4) or $Co_xO_ySi_z$ moieties, as reported by Lim et al. [34]. TPR results are in agreement with this possibility since it has been shown in Table 3 that the amount of non-exchanged Co species decreases when silica is present in the slurry. This fact suggests the formation of silicates whose reduction temperature is higher than that of cobalt oxides. Puskas et al. [35] reported that cobalt silicate during the preparation or treatment of Co/SiO_2 is the result of a facile chemical reaction between hydrated cobalt hydroxide and silicic acid. In our case, this reaction can occur if the reagents are generated simultaneously during the chemical reaction under wet conditions and this fact explains why silica is beneficial only in this case. At this point, a question arises: if cobalt silicate species are formed only under wet conditions, why during the TPR experiments does the hydrogen consumption in the zone of cobalt oxides decrease not only after wet reaction but also after calcination in dry oxygen? This can be explained taking into account that during TPR water is formed, thus cobalt silicates would be formed in situ. Unfortunately, the amount of silica added as a binder is too small (1 wt.%) and cobalt silicate species cannot be detected by the characterization technique used in this work. TPR peaks of cobalt silicates appear in the 400–800 °C range which is in agreement with those of exchanged Co^{+2} which occur in the high-temperature zone (700–900 °C) and Co oxide species (200–600 °C). On the other hand, Raman bands of silicates overlap with mordenite ones.

Despite the above-mentioned difficulties in characterizing cobalt silicates, by combining TPR, UV–vis and Raman data, their presence can be indirectly inferred in the monolithic catalyst irreversibly deactivated after 10 h of time-on-stream with 10% of water in the feed. Raman results show that a strong signal at 690 cm^{-1} develops for the deactivated catalyst, which corresponds to Co_3O_4. UV–vis results also show the signal characteristics of Co_3O_4, while those of exchanged Co^{+2} almost disappear. For the same solid, the TPR profile shows a strong peak at 391 °C which corresponds to Co_3O_4 and a smaller one at 847 °C. The latter peak could be attributed either to exchanged Co^{+2} or $CoSiO_4$. Since exchanged cobalt is practically not shown in the UV–vis spectra, the TPR peak would be attributed, at least in part, to cobalt silicate.

4. Conclusions

When the amount of water is low (2%) the positive or negative effect on the NO_x SCR depends on the reductant used. When methane is the hydrocarbon, water decreases the NO_x conversion because it inhibits the NO_x adsorption on the active sites. However, when butane is used, water (2%) increases the NO_x conversion because its positive effect of maintaining the surface clean of carbon deposits prevails over the adsorption inhibition. The cleaning effect was confirmed by TPO and XPS techniques. More rigorous reaction conditions, i.e., dry/wet cycles with 10% of water lead to irreversible deactivation for both reductants. These are common facts in both powder and monolithic catalysts.

For monolithic catalysts washcoated with Co-mordenite, the silica binder effect is positive under wet conditions but the opposite occurs in the absence of water. The hydrogen binding of zeolite crystals with fumed silica and/or the reaction of silica with deleterious cobalt oxide species to give Co_2SiO_4 crystals or $Co_xO_ySi_z$ moieties could be the reason for the positive effect. On the other hand, fumed silica particles can obstruct reactant diffusion under dry conditions. Characterization results (TPR, LRS, UV–vis) indicate that in deactivated catalysts the main cobalt species is Co_3O_4.

Acknowledgments

The authors wish to acknowledge the financial support received from UNL, CONICET and ANPCyT. They are also grateful to Dr. Angel Martínez-Hernández and Dr. Gustavo Fuentes Zurita of "Area de Ingeniería Química" Universidad Autónoma Metropolitana-Iztapalapa, México, for their assistance in the DRS measurements. Thanks are finally given to Prof. Elsa Grimaldi for the English language editing and to ANPCyT for Grant PME 8—2003 to finance the purchase of the UHV multi analysis system.

References

[1] V.I. Parvulescu, P. Grange, B. Delmon, Catal Today 46 (1998) 223.
[2] H.Y. Chen, X. Wang, W.M.H. Sachtler, Appl. Catal. A 194/195 (2000) 159.
[3] A. Kubacka, J. Janas, E. Wloch, B. Sulikowski, Catal Today 101 (2005) 139.
[4] Y. Li, J.N. Armor, Appl. Catal. B 1 (1992) L31.
[5] T. Maunula, J. Ahola, H. Hamada, Appl. Catal. B 64 (2005) 13.
[6] F. Zhang, S. Zhang, N. Guan, E. Schreier, M. Richter, R. Eckelt, R. Fricke, Appl. Catal. B 73 (3/4) (2007) 209.
[7] R. Burch, J.P. Breen, F.C. Meunier, Appl. Catal. B 39 (2002) 283.
[8] J. Armor, Catal Today 26 (1995) 147.
[9] L. Gutierrez, M.A. Ulla, E.A. Lombardo, A. Kovacs, F. Lonyi, J. Valyon, Appl. Catal. A 292 (2005) 154.
[10] H.-Y. Chen, Q. Sun, B. Wen, Y.-H. Yeom, E. Weitz, W.M.H. Sachtler, Catal. Today 96 (2004) 1.
[11] M.V. Twigg, Appl. Catal. B 70 (2007) 2.
[12] Y. Li, J.N. Armor, Appl. Catal. B 2 (1993) 239.
[13] Y. Li, J.N. Armor, J. Catal. B 150 (1994) 376.
[14] E.M. Sadovskaya, A.P. Suknev, L.G. Pinaeva, V.B. Goncharov, B.S. Balázhinimaev, C. Chupin, J. Pérez-Ramírez, C. Mirodatos, J. Catal. 225 (2004) 179.
[15] M.C. Campa, I. Luisetto, D. Pietrogiacomi, V. Indovina, Appl. Catal. B 46 (2003) 511.
[16] A. Boix, E.E. Miró, E.A. Lombardo, M.A. Bañares, R. mariscal, J.L.G. Fierro, J. Catal. 217 (2003) 186.
[17] A. Martínez-Hernández, G. Fuentes, Appl. Catal. B 57 (2005) 167.
[18] P. Avila, M. Montes, E. Miro, Chem. Eng. J. 109 (2005) 11.
[19] S. Akaratiwa, T. Nanba, A. Obuchi, J. Okayasu, J.O. Uchisawa, S. Kushiyama, Top. Catal. 16/17 (1–4) (2001) 209.
[20] Z.R. Ismagilov, R.A. Shkrabina, L.T. Tsykoza, V.A. Sazonov, S.A. Yashnik, V.V. Kuznetsov, N.V. Shikina, H.J. Veringa, Top. Catal. 16/17 (1–4) (2001) 307.
[21] A. Boix, J.M. Zamaro, E. Lombardo, E. Miro, Appl. Catal. B 46 (2003) 121.
[22] A. Boix, E. Miró, E.A. Lombardo, R. Mariscal, J.L.G. Fierro, Appl. Catal. A 276 (2004) 197.
[23] L. Li, J. Chen, S. Zhang, N. Guan, M. Richter, R. Eckelt, R. Fricke, J. Catal. 228 (2004) 12.
[24] J.M. Zamaro, M.A. Ulla, E.E. Miró, Chem. Eng. J. 106 (2005) 25.
[25] L. Gutierrez, A. Boix, J. Petunchi, J. Catal. 179 (1998) 179.
[26] B. Jongsomjit, J.G. Goodwin Jr., Catal. Today 77 (2002) 191.
[27] Z. Sobalík, J. Dědeček, D. Kaucký, B. Whichterlová, L. Drozdová, R. Prins, J. Catal. 194 (2000) 330.
[28] J. Dědeček, B. Whichterlová, J. Phys. Chem. B 103 (1999) 1462.
[29] F.E. Triguero, C.M. Ferreira, J.-C. Volta, W.A. Gonzales, P.G. Pries de Oliveria, Catal. Today 118 (2006) 425.
[30] S. Lim, D. Ciuparu, C. Pak, F. Dobek, Y. Chen, D. Harding, L. Pfefferle, G. Haller, J. Phys. Chem. B 107 (2003) 11048.
[31] C. Chupin, A.C. van Veen, M. Konduru, J. Després, C. Mirodatos, J. Catal. 241 (2006) 103.
[32] A. Shichi, Y. Kawamura, A. Satsuma, T. Hattori, Stud. Surf. Sci. Catal. 135 (2001) 4876.
[33] X. Chen, A.R. Tadd, J.W. Schwank, J. Catal. 251 (2007) 374.
[34] S. Lim, C. Wang, Y. Yang, D. Ciuparu, L. Pfefferle, G. Haller, Catal. Today 123 (2007) 122.
[35] I. Puskas, T.H. Fleisch, J.A. Kaduk, C.L. Marshall, B.L. Meyers, M.J. Catagnola, J.E. Indacochea, Appl. Catal. A 316 (2007) 197.